

Flow Properties of Saturated Rubber-Modified Polymer Melts

KUNIYOSHI ITOYAMA and ATSUHIKO SODA, *Plastics Research Laboratories, Toray Industries, Inc., Otsu, Shiga, Japan*

Synopsis

The flow properties of saturated rubber-modified polymer melts were studied using a capillary rheometer. The two-phase polymer consists of styrene-acrylonitrile copolymer as matrix and ethylene-vinyl acetate copolymer (EVA) as rubber component. When the rubber concentration increases, melt viscosity of the polymer increases appreciably and activation energy for the viscous flow decreases. When the degree of grafting of EVA rubber increases, melt viscosity of the polymer increases, but activation energy is nearly constant at a given shear rate. It is shown that the superposition principle of shear rate-temperature is applicable to polymer containing from 0 to 12 wt-% rubber at a temperature from 180 to 280°C and that the superposition principle of shear rate-concentration is also applicable only in the shear rate range of above 70 sec^{-1} . Die swell ratio decreases monotonically with increasing rubber concentration. A master curve is obtained for the reduced variables of die swell ratio and shear rate using the method described by Petraglia et al. Assuming the polymer melt as a generalized Maxwell body, relaxation spectra were evaluated from die swell ratio and dependence of viscosity on shear rate.

INTRODUCTION

Toughening of a normally brittle glassy polymer by incorporation of dispersed rubbery particles is successfully established in many ways. Polymers containing polybutadiene or unsaturated rubber, such as high-impact polystyrene (HIPS) and ABS polymers, are commercially important polymers which show excellent impact strength, but these polymers have poor weather resistance.

A saturated rubber-modified polymer, which is a polymer consisting of styrene-acrylonitrile copolymer (SAN) as continuous phase and ethylene-vinyl acetate copolymer (EVA) as dispersed rubbery phase (the polymer is hereafter referred to AES), has been developed recently in order to improve weather resistance.¹⁻⁴ In this polymer, the EVA rubber particles are stably dispersed in the SAN medium due to the affinity for SAN grafted to rubber molecules. However, the molecular structure of EVA particles is very different from that of unsaturated rubber particles, e.g., the degree of crosslinkage of rubber particles is lower in the AES polymer than in ABS and HIPS, and also the density of the graft polymers likely located at the interface with the continuous phase is less in the AES polymer. These molecular structural features of the AES polymer produce practical differences in various processings or mechanical properties from unsaturated rubber-modified polymers.

This report describes the effects of EVA rubber particles on rheological properties such as steady flow and Barus effect of molten AES polymers.

EXPERIMENTAL

Preparation of AES Polymers

Preactivation of Rubber

Ethylene-vinyl acetate copolymer (EVA) used was Evaflex 560 (melt index 3.5 g/10 min; VAc content, 14 wt-%) purchased from Mitsui Polychemical Co. EVA was chemically modified by ester interchange with methyl methacrylate (MMA) to introduce pendent unsaturated groups for the purpose of grafting and crosslinking. Ester interchange was conducted by dissolving 20 parts EVA in 71 parts styrene and by reacting with 9 parts MMA in the presence of sodium methylate-methanol solution and hydroquinone as polymerization inhibitor. The reaction was carried out with agitation at 75°C for 1 to 3.5 hr. The ester-interchanged (preactivated) EVA was analyzed by iodine titration of methacrylic acid (MAA) after hydrolysis by potassium hydroxide. Seven samples of preactivated EVA having 0.06 to 0.45 mmole MAA per 1 g EVA were prepared; and by using these EVA samples, AES polymers having different degrees of grafting were polymerized by the following procedures.

Bulk Suspension Polymerization

In a reactor, preactivated EVA containing 12 parts EVA was dissolved in 62.4 parts styrene and 18.6 parts acrylonitrile. The batch was charged with *tert*-dodecylmercaptan and azobisisobutyronitrile, and polymerization was carried out by stirring at 75°C. Bulk polymerization was continued for 3 to 4 hr. Phase inversion occurred after 2.6 to 3 hr, and the rubbery phase was dispersed in the continuous phase of SAN. Then, 200 parts aqueous solution containing suspending agent, poly(butyl acrylate), was charged to obtain a suspension, and polymerization was continued at 50 to 115°C for 3.5 hr. The resulting polymers were washed with water and dried in vacuo.

Samples for Test

Five samples having rubber concentrations from 0 to 12 wt-% were prepared by the following procedure. An AES polymer containing 12 wt-% rubber, polymerized initially, was blended with SAN to obtain polymers containing 3, 6, and 9 wt-% rubber, and dry-blended polymers were pelletized at 180°C by using an extruder. Weight-average molecular weight of the blending SAN was so adjusted as to be almost the same as that of SAN in AES polymers. SAN was extracted from AES polymers by using tetrahydrofuran and analyzed to contain 24 wt-% acrylonitrile units. Molecular characteristics of SAN were determined by gel permeation chromatography and viscometry. Characteristics of SAN and AES polymers are shown in Table I.

Measurement of Flow Properties

Measurements of melt flow were made using a capillary rheometer at temperatures from 180 to 280°C. Three flate-entry capillaries having a diameter d of 1.0 mm and lengths l of 1, 5, and 10 mm, and a fourth capillary of diameter 0.5 mm and length 20 mm were used for all flow measurements. Maximum shear

TABLE I
Characterization of AES Polymers

Sample no.	Chemical properties						Mechanical properties ^b	
	Continuous phase			Dispersed phase			Tensile yield strength, ^c kg/cm ²	Izod impact strength, ^d kg cm/cm ²
	AN %	$M_w \times 10^{-4}$	M_w/M_n	Rubber conc., wt-%	Particle diam., ^a μm	MAA content in preactivated EVA, mmole/g EVA		
AES-1	24	16.7	2.7	12	1~3	0.26	446	8.5
AES-2	24	16.7	3.0	9	1~3	0.26	520	6.0
AES-3	24	16.7	3.3	6	1~3	0.26	580	5.0
AES-4	24	16.7	3.6	3	1~3	0.26	640	2.0
AES-5	24	16.7	3.9	0	—	—	—	—
AES-6	24	17.1	2.6	12	2~6	0.06	520	5.3
AES-7	24	17.1	2.7	12	1.4~6	0.10	480	6.5
AES-8	24	17.1	2.7	12	1~4	0.15	460	7.0
AES-9	24	17.1	2.5	12	1~3	0.21	455	8.0
AES-10	24	17.1	2.9	12	1~3	0.26	450	8.0
AES-11	24	17.1	2.6	12	0.6~3	0.45	430	5.6

^a Particle size was measured by means of transmission electron microscopy using the Kato osmium staining technique.²⁰

^b Obtained by compression molding.

^c ASTM D 638.

^d ASTM D 256.

stresses τ_w at the wall were corrected according to Bagley's method, and shear rates $\dot{\gamma}_w$ were calculated at the wall, corrected according to the Rabinowitsch-Mooney relation. Apparent viscosities were calculated from the equation $\eta_a = \tau_w / \dot{\gamma}_w$. Maximum diameters of die swelling of polymer melts, d_{\max} , were measured by using an optical microscope of magnification of 20.

RESULTS AND DISCUSSION

Effect of Dispersed Rubbery Particles on Melt Viscosity

The influence of the rubber on the melt viscosity of AES polymers is shown in Figure 1 at different shear rates and stresses. For dispersed systems of spherical particles, the relative viscosity η_r may be expressed at a relatively low shear rate and stress in the following Mooney-type equation⁵:

$$\eta_r = \frac{(\eta_a)_F}{(\eta_a)_0} = \exp \frac{2.5\sigma\phi_F}{1 - k\sigma\phi_F} \quad (1)$$

where ϕ_F is the volume fraction of filler, σ is the apparent expansion coefficient of the filler volume, k is a constant, and the subscripts F and zero refer to the filled and unfilled systems, respectively.

No attempt has been made to extrapolate η_r to zero shear; instead, data obtained to 3.0 sec^{-1} and $1.23 \times 10^5 \text{ dynes/cm}^2$ were used directly. Equation (1) is plotted as curves in Figure 1. The estimated values of σ at a shear rate of 3 sec^{-1} and at a shear stress of $1.23 \times 10^5 \text{ dynes/cm}^2$ are 2.0 and 2.2, respectively. This fact indicates that the apparent volume of dispersed rubber in AES melts is about 2.0 times as large as the real volume of rubber. Further, the deviation

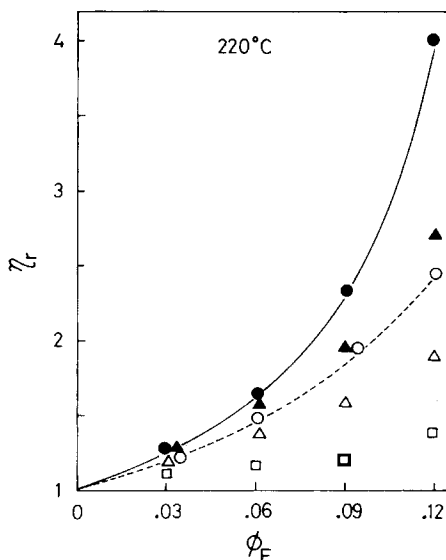


Fig. 1. Relative apparent viscosity vs weight fraction rubber at constant shear rates of 3 sec^{-1} (○), 10^{-1} sec^{-1} (△), and 100 sec^{-1} (□), and at shear stresses of $1.23 \times 10^6 \text{ dynes/cm}^2$ (●) and $1.84 \times 10^6 \text{ dynes/cm}^2$ (▲). Curves represent eq. (1) with $\sigma = 2.2$, $k = 1.9$ (—), and $\sigma = 2.0$, $k = 1.4$ (- -).

from the simple Einstein relation with increasing rubber concentration suggests a strong interaction of rubber particles, requiring the need for higher terms in the concentration. The decrease in relative viscosity with increasing shear rate, shown in Figure 1, is consistent with the behavior reported by Mill,⁶ who studied the effects of glass spheres in a polystyrene melt.

Temperature dependence of melt viscosity is often expressed by means of the Arrhenius equation. Two different activation energies for the relative viscosity of non-Newtonian fluids can be defined as follows: (1) activation energy at constant shear stress τ_w : $\Delta E_{\tau_w} = -(E_0 - E_F)_{\tau_w}$ and (2) activation energy at constant shear rate $\dot{\gamma}_w$: $\Delta E_{\dot{\gamma}_w} = -(E_0 - E_F)_{\dot{\gamma}_w}$. Although ΔE_{τ_w} and $\Delta E_{\dot{\gamma}_w}$ differ from each other, $\Delta E_{\tau_w} = \Delta E_{\dot{\gamma}_w}$ at zero shear.

ΔE_{τ_w} and $\Delta E_{\dot{\gamma}_w}$ were obtained from the plot of $\log \eta_r$ versus $1/T$ at constant shear stress and shear rate, respectively. On the assumption that rubber particles make no contribution to the flow activation energy, the activation energy is related by the following equation:

$$\frac{E_0 - E_F}{\phi_F} = \sigma E_0 \quad (2)$$

$-\Delta E_{\tau_w}/\phi_F$ and $-\Delta E_{\dot{\gamma}_w}/\phi_F$ were plotted as a function of rubber fraction, as shown in Figure 2. It is obvious from Figure 2 that eq. (2) approximately holds for each shear stress and shear rate. A similar dependence of activation energy on the fraction of dispersed particles was observed for ABS polymers^{7,8} and polystyrene latex.⁹ The activation energies of unfilled and filled systems decrease with increasing shear rate, and the estimated values of σ change from 1.5 to 3.6 according to the flow condition. The values of σ , estimated at constant shear stresses, almost coincide with the values from the relative viscosity.

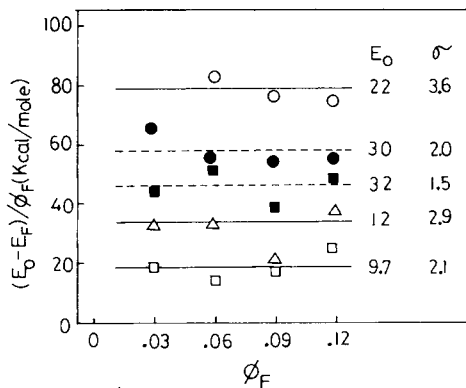


Fig. 2. Adjusted activation energy difference vs weight fraction of rubber at constant shear rates of 50 sec^{-1} (O), 10^3 sec^{-1} (Δ) and 10^4 sec^{-1} (\square), and at constant shear stresses of $1.23 \times 10^5 \text{ dynes/cm}^2$ (\blacksquare) and $1.84 \times 10^6 \text{ dynes/cm}^2$ (\bullet). Values of σ were estimated by eq. (2).

Such variation of activation energy suggests that the dispersed rubbers are merely an extending filler for the medium and make almost no contribution to the temperature dependence of the viscosity. In other words, the variation can probably be attributed to the decrease in molecular polarity or molecular entanglement density of the medium component with increasing the rubber particles.

Effect of Graft SAN on Melt Viscosity

The rubber particle size of AES polymer decreases as the content of MAA in the preactivated EVA rubber increases, as shown in Table I. Figure 3 shows plots of apparent melt viscosity η_a versus MAA content. A marked increase in viscosity is observed at 3 sec^{-1} , but at 100 sec^{-1} η_a increases slightly with increase in MAA content and keeps nearly constant at MAA contents above about 0.22

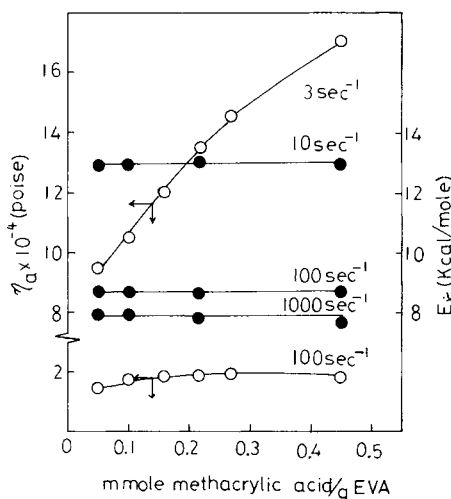


Fig. 3. Apparent viscosity (at 220°C) and activation energy as a function of the methacrylic acid content at constant shear rates.

mmole MAA per 1 g EVA. This agrees almost with the region in which the rubber particle size remains nearly constant.

The activation energies for melt flow at constant shear rate, $E_{\dot{\gamma}_w}$, are plotted in Figure 3 as functions of MAA content. The $E_{\dot{\gamma}_w}$ value remains unchanged, and the values of $E_{\dot{\gamma}_w}$ are 13, 8.6, and 7.9 kcal/mole at a shear rate 10, 100, and 1000 sec^{-1} , respectively. This fact is quite different from the case of increasing the rubber concentration. It is suggested from Figure 3 that the activation energy does not depend on such factors as the content of graft SAN and the size of the rubber particles but somewhat on the rubber content. Therefore, it may be said that grafting has more effect on the viscosity than on the activation energy.

Superposition of Flow Curves

The applicability of the superpositions of temperature–time and concentration–time was examined for AES polymers having various rubber concentrations. An arbitrary reference temperature, T_R , of 220°C was chosen, and for each sample the logarithmic shear stress–shear rate flow curves at various temperatures T were shifted to superimpose on the reference temperature curve using the shift factor a_T defined as

$$a_T = \dot{\gamma}_w(T_R)/\dot{\gamma}_w(T) \quad (3)$$

The results of temperature–time superposition are illustrated in Figure 4. Excellent superposition can be observed for AES-1, AES-3, and AES-5, and this was the case for all other samples listed in Table I. It is well known that in homopolymer, flow curves for different temperatures can be superimposed. Also the same procedure can be applied to ABS polymers.^{8,10}

These results of two-phase polymers suggest that the relaxation times corresponding to the cooperative motional modes may have the same temperature dependence for dispersed particle–medium systems.

Figure 4 also shows that a_T approximately conforms to an Arrhenius-type

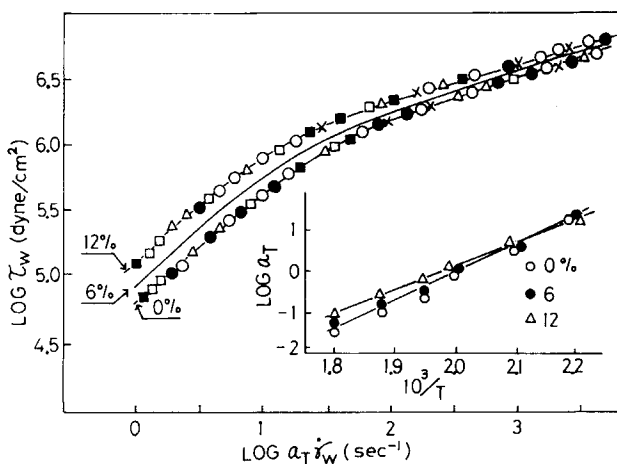


Fig. 4. Master flow curves reduced at 220°C and Log a_T vs $1/T$ for AES polymers of different rubber concentrations: (X) 180°C; (O) 200°C; (●) 220°C (ref. temp.); (Δ) 240°C; (□) 260°C; (■) 280°C.

equation. The activation energies obtained from a_T are 32, 28, and 26 kcal/mole for 0, 6, and 12 wt-% rubber, respectively. These activation energies correspond to those at constant shear stress and coincide with those obtained from viscosity at the relatively low shear stress of 1.23×10^5 dynes/cm². Kubota¹¹ obtained 32.2 kcal/mole through the extrapolation of shear stress to zero for SAN polymers. It agrees well with the value obtained from a_T .

Figure 5 shows the superposition of concentration-time at 220°C. The shift factor a_c in this case was defined as

$$a_c = \dot{\gamma}_w(0)/\dot{\gamma}_w(C) \quad (4)$$

where $\dot{\gamma}_w(0)$ and $\dot{\gamma}_w(C)$ are the shear rate at the concentration of 0 and C wt-%, respectively. The superposition constructs a master flow curve at shear rates above 70 sec^{-1} , while at lower shear rates the superposition fails appreciably. The rubber is seen to have a noticeable effect on the shear rate dependence of shear stress with considerable divergence occurring at low shear rates.

Figure 5 shows that the dependence of a_c on ϕ_F is expressed as

$$a_c = \exp(5.0\phi_F) \quad (5)$$

For the case of low rubber concentration with negligibly small interaction between rubber particles, eq. (5) is rewritten as

$$a_c = 1 + 5.0\phi_F \quad (6)$$

By assuming that at low rubber concentration at which eq. (6) holds, the concentration-time superposition can be extensively applied to the Newtonian region of the medium, the constant of ϕ_F in eq. (6) is 2.0 times larger than Einstein's constant 2.5, and it corresponds to the apparent increase of 2.0 times the effective volume of rubber particles. This result agrees well with that obtained at constant shear stress from viscosity and activation energy.

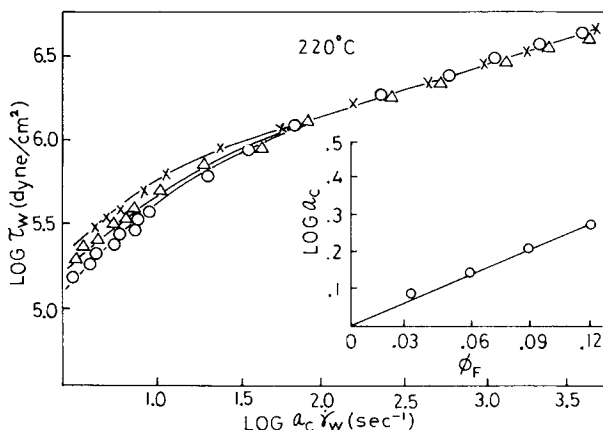


Fig. 5. Master flow curves reduced to 0 wt-% of rubber and shift factor a_c vs weight fraction rubber: (x) 12 wt-%; (Δ) 6 wt-%; (O) 0 wt-%.

Barus Effect in AES Melts

When polymer melts are extruded from a capillary, the diameter of the extrudate is larger than that of the capillary. The phenomenon is attributed to the elastic properties of polymer melts.^{12,13} Assuming that the elastic deformation of polymer melts at the capillary inlet and the relaxation of the elastic deformation in the capillary are the dominating factors for the die swelling, we introduce the following two parameters according to Petraglia et al.¹⁴:

$$\beta = [1 - (d/d_{\max})^2]/[1 - (d/d_0)^2] \quad (7)$$

$$\bar{t}_r = 8l/d_0\dot{\gamma}_w a_T \quad (8)$$

where d , d_0 , and d_{\max} are the diameter of the capillary, the diameter of the reservoir, and the maximum diameter of polymer stream due to die swelling, respectively; l is the length of the capillary; a_T is the shift factor of the temperature-time superposition; and β and \bar{t}_r indicate the ratio of the expansion ratio to the compression ratio and the reduced residence time of the polymer melts in the capillary, respectively.

Figure 6 shows plots of β versus $\log \bar{t}_r$ for AES polymers having different rubber concentrations. It is clear that at the same rubber concentrations the data with various l/d , shear rates, and temperatures agree well with the master curve. Also, the plots of β versus $\log \bar{t}_r$ give a nearly straight line having a slope of -0.2 in every system.

The viscosity η_F and the shear modulus G_F of systems containing filler are related to the quantities for the unfilled matrix η_0 , G_0 by $\eta_F/\eta_0 = G_F/G_0$.¹⁵ Therefore, as the viscosity goes up in the rubber-modified systems, so does the shear modulus, and the swelling decreases with increasing rubber concentration, as reported for polymers filled with inorganic particles.¹⁶

Next, by assuming that the molten AES is a generalized Maxwell body, the relaxation spectra can be predicted from the following equation¹⁴:

$$H(\tau) = -(\eta_N/\tau)[d\beta/d(\ln \bar{t}_r)]_{\bar{t}_r=\tau} \quad (9)$$

where τ is the relaxation time and η_N is the Newtonian viscosity at low shear rate. The flow of AES can be described by the following modified Cross equation¹⁷:

$$(\eta_N - \eta_a)/\eta_a = \alpha \dot{\gamma}_w^{0.78} \quad (10)$$

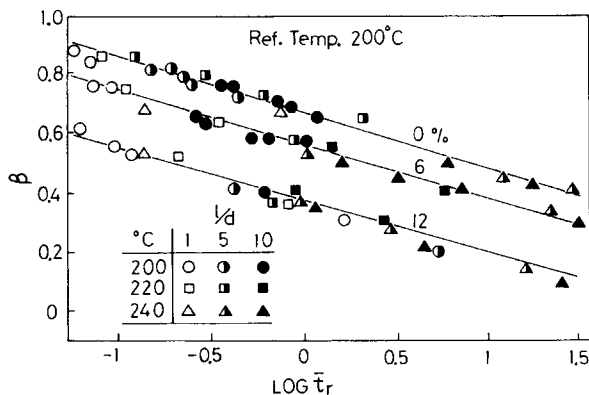


Fig. 6. Plot of swelling parameter β vs reduced capillary residence \bar{t}_r for AES polymers containing 0, 6, and 12 wt-% rubber.

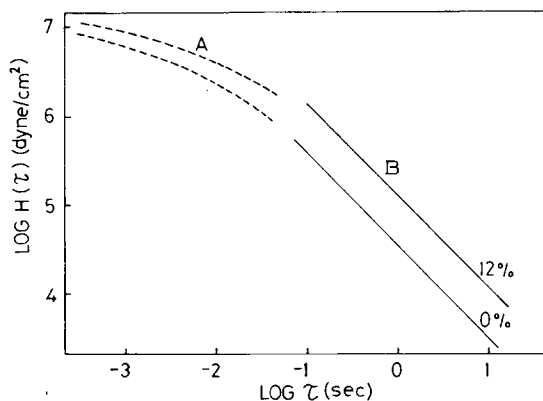


Fig. 7. Relaxation spectrum $H(\tau)$ as function of relaxation time τ for AES polymers containing 0 and 12 wt-% rubber: A, flow curve; B, swelling.

where α is a constant. η_N was estimated from the viscosity–shear rate relation in the non-Newtonian region by using eq. (10). The η_N values of AES containing 0 and 12 wt-% rubber were 4.7×10^4 and 5.0×10^5 poises at 200°C, respectively. In Figure 7, $H(\tau)$ is plotted versus τ for AES containing 0 and 12 wt-% rubber at the reference temperature of 200°C. The same relaxation spectrum can be derived analytically from plots of viscosity versus shear rate by using the following equation¹⁴:

$$H(\tau) = \frac{1}{\tau} \left[\eta_a d(\ln \eta_a) / d(\ln \dot{\gamma}_w) \right]_{\dot{\gamma}_w = 1/\sqrt{8}\tau} \quad (11)$$

Figure 7 shows the relaxation spectrum versus τ obtained by the flow curve. There is good agreement between the two curves calculated from the flow curve and die swelling. It is also shown that the two-phase polymer containing rubber has a somewhat higher intensity of the relaxation spectrum at long relaxation times than SAN. This indicates that the presence of EVA rubber in the AES polymer has an influence on the viscoelasticity of the polymer in that it extends the width of the rubbery plateau region of the relaxation spectrum. The same result has been suggested for ABS polymers from the measurement of tensile relaxation moduli by Scalco et al.¹⁹

The authors express their appreciation to the manager of Toray Industries, Inc., for permission to publish this paper and to Dr. K. Kato and T. Nishdoi for helpful discussions during the course of this investigation.

References

1. M. Baer, *J. Appl. Polym. Sci.*, **16**, 1125 (1972).
2. S. Koiwa, *J. Appl. Polym. Sci.*, **19**, 1625 (1975).
3. K. Ousima and H. Kiuchi; Toray Industries, Inc. Jap. Pat. No. 13353 (1973).
4. K. Ousima, T. Aoyama, and H. Kiuchi; Toray Industries, Inc. Jap. Pat. No. 13349 (1973).
5. M. Mooney, *J. Colloid Sci.*, **6**, 162 (1951).
6. N. J. Mills, *J. Appl. Polym. Sci.*, **15**, 2791 (1971).
7. M. G. Hugué and T. R. Paxton, *Am. Chem. Soc., Div. Polym. Chem., Prepr.*, **2**, 548 (September 1970).
8. K. Itoyama and A. Soda, *Kobunshi Ronbunshu (Soc. Polym. Sci. Japan)*, **33** (8), 471 (1976).
9. S. H. Maron and S. M. Fok, *J. Colloid Sci.*, **10**, 482 (1955).

10. R. A. Mendelson, *Polym. Eng. Sci.*, **16**, 690 (1976).
11. H. Kubota, *J. Appl. Polym. Sci.*, **19**, 2299 (1975).
12. E. B. Bagley and H. J. Duffey, *Trans. Soc. Rheol.*, **14**, 545 (1970).
13. Y. Mori and K. Funatsu, *Appl. Polym. Symp.*, **No. 20**, 209 (1973).
14. G. Petraglia and A. Coen, *Polym. Eng. Sci.*, **10**(2), 79 (1970).
15. L. E. Nielsen, *J. Composite Mater.*, **1**, 100 (1967).
16. S. Newman and Q. A. Trementozzi, *J. Appl. Polym. Sci.*, **9**, 3071 (1965).
17. M. M. Cross, *J. Colloid Sci.*, **20**, 417 (1965).
18. E. Scalco, T. W. Huseby, and L. L. Blyler, *J. Appl. Polym. Sci.*, **12**, 1343 (1968).
19. K. Kato, *J. Electron Microscopy*, **14**, 220 (1965).

Received May 24, 1977

Revised April 28, 1978